

Accurate Computation of the Trajectory of the Spin and Fin-Stabilized Projectiles

Dimitrios N. Gkritzapis, Elias E. Panagiotopoulos

Abstract— The modified projectile linear theory trajectory report here will prove useful to estimate trajectories of high spin and fin-stabilized projectiles. The model of the modified linear theory is compared with a 6-DOF trajectory model. The computational flight analysis takes into consideration all the aerodynamics variations by means of the variable aerodynamic coefficients. Static stability, also called gyroscopic stability, is examined. The developed computational method gives satisfactory agreement with published experimental data and computational codes for atmospheric projectile trajectory analysis with various initial firing flight conditions.

Keywords— Rapid trajectory prediction, Projectile motion, Modified linear model, Variable aerodynamic coefficients.

I. INTRODUCTION

External ballistics [1] deals with the behavior of a non-powered projectile in flight. Several forces act the projectile during this phase including gravity and air resistance.

The pioneering British ballisticians Fowler, Gallop, Lock and Richmond [2] constructed the first rigid six-degree-of-freedom projectile exterior ballistic model. Various authors have extended this projectile model for lateral force impulses [3]-[4], proposed linear theory in atmospheric flight for dual-spin projectiles [5]-[6], as well as aerodynamic jump extending analysis due to lateral impulsives [7] and aerodynamic asymmetry [8], instability of controlled projectiles in ascending or descending flight [9]. Costello's modified linear theory [10] has also applied recently for rapid trajectory projectile prediction.

The present work proposes several modifications to full six degrees of freedom (6-DOF) theory that significantly improve accuracy of impact point prediction of short and long range trajectories with variable aerodynamic coefficients of high spin and fin-stabilized projectiles, while still maintaining low computation cost for real-time implementation of a smart weapon control law. For the purposes of the analysis, linear interpolation has been applied from the tabulated database of

This work was supported in part by the Hellenic Military Academy.

Dr Dimitrios N. Gkritzapis, lecturer in Hellenic Military Academy and Captain of Hellenic Police in the Laboratory of Firearms and Tool Marks Section, Criminal Investigation Division, Hellenic Police, 11522 Athens, Greece (e-mail: gritzap@yahoo.gr).

Dr. Elias. P. Panagiotopoulos lecturer in Hellenic Military Academy, (email: hpanagio@mech.upatras.gr).

McCoy's text [1]. The efficiency of the developed method gives satisfactory results compared with published data of verified experiments and computational codes on dynamics model analysis of short and long-range trajectories of spin and fin-stabilized projectiles.

The present analysis considers two different types of representative projectiles. A typical formation of the cartridge 105mm HE M1 projectile is, and is used with various 105mm howitzers. And the 120 mm Mortar System provides an organic indirect-fire support capability to the manoeuvre unit commander. Basic physical and geometrical characteristics data of the above-mentioned 105 mm HE M1 projectile and the non-rolling, finned 120 mm HE mortar projectile illustrated briefly in Table 1.

Characteristics	105 mm	120 mm
Reference diameter, mm	104.8	119.56
Total length, mm	494.7	704.98
Weight, kg	15.00	13.585
Axial moment of inertia, $\text{kg}\cdot\text{m}^2$	$2.32\cdot 10^{-2}$	$2.33\cdot 10^{-2}$
Transverse moment of inertia, $\text{kg}\cdot\text{m}^2$	$2.31\cdot 10^{-1}$	$2.31\cdot 10^{-1}$
Center of gravity from the base, mm	183.4	422.9

Table 1. Physical and geometrical data of 105 mm and 120mm projectiles types.

II. TRAJECTORY FLIGHT SIMULATION MODEL

A six degree of freedom rigid-projectile model [11-14] has been employed in order to predict the "free" nominal atmospheric trajectory to final target area without any control practices. The six degrees of freedom flight analysis comprise the three translation components (x , y , z) describing the position of the projectile's center of mass and three Euler angles (ϕ , θ , ψ) describing the orientation of the projectile body with respect to Fig.1.

Two main coordinate systems are used for the computational approach of the atmospheric flight motion. The one is a plane fixed (inertial frame, IF) at the firing site. The other is a no-roll rotating coordinate system on the projectile body (no-roll-frame, NRF, $\phi = 0$) with the X_{NRF} axis along the projectile axis of symmetry and Y_{NRF} , Z_{NRF} axes oriented so as to complete a right hand orthogonal system. The twelve state variables x , y , z , ϕ , θ , ψ , u , v , w , p , q and r are necessary to

describe position, flight direction and velocity at every point of the projectile's atmospheric flight trajectory. Introducing the components of the acting forces and moments expressed in the no-roll-frame (\sim) rotating coordinate system with the dimensionless arc length s as an independent variable, the following full equations of motion for six-dimensional flight are derived:

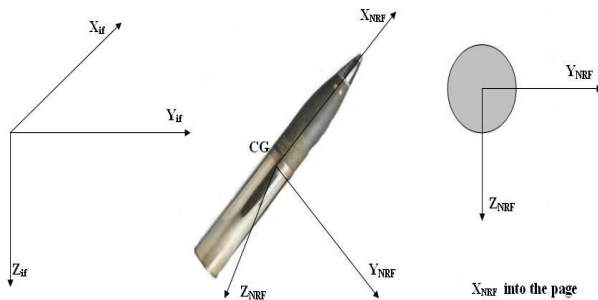
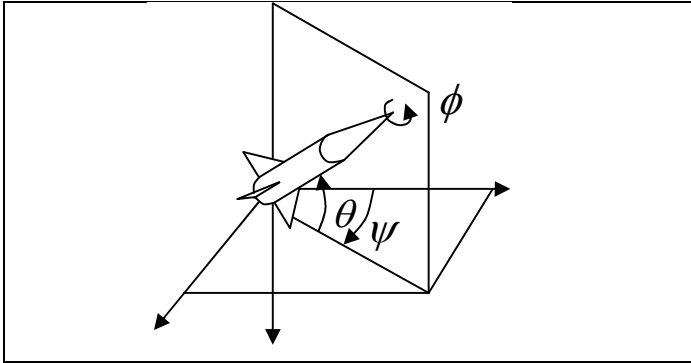


Figure 1. No-roll (moving) and earth-fixed (inertial) coordinate systems for the projectile trajectory analysis with the corresponding orientation definitions (Euler angles).

$$x' = D \cos \psi \cos \theta - \frac{D}{V} \sin \psi \tilde{v} + \tilde{w} \cos \psi \sin \theta \frac{D}{V} \quad (1)$$

$$y' = D \cos \theta \sin \psi + \tilde{v} \cos \psi \frac{D}{V} + \tilde{w} \sin \theta \sin \psi \frac{D}{V} \quad (2)$$

$$z' = -D \sin \theta + \frac{D}{V} \tilde{w} \cos \theta \quad (3)$$

$$\phi' = \frac{D}{V} \tilde{p} + \frac{D}{V} \tan \theta \tilde{r} \quad \theta' = \frac{D}{V} \tilde{q} \quad \psi' = \frac{D}{V \cos \theta} \tilde{r} \quad (4, 5, 6)$$

$$\begin{aligned} \tilde{u}' = & -\frac{D}{V} g \sin \theta - K_I V C_X - K_I V C_X^2 \alpha^2 - K_I V C_X^2 \beta^2 + \\ & + \tilde{v} \frac{D}{V} \tilde{r} - \tilde{q} \frac{D}{V} \tilde{w} \end{aligned} \quad (7)$$

$$\begin{aligned} \tilde{v}' = & -K_I C_{NA} (\tilde{v} - \tilde{v}_w) + D \frac{K_I}{2} \tilde{p} C_{MaF} \alpha - \frac{D}{V} \tilde{r} \tilde{w} \tan \theta - \\ & - D \tilde{r} \end{aligned} \quad (8)$$

$$\begin{aligned} \tilde{w}' = & \frac{D}{V} g \cos \theta - K_I C_{NA} (\tilde{w} - \tilde{w}_w) - \\ & - D \frac{K_I}{2} \tilde{p} C_{MaF} \beta + D \tilde{q} + \tan \theta \frac{D}{V} \tilde{r} \tilde{v} \end{aligned} \quad (9)$$

$$\tilde{p}' = D^5 \frac{\pi}{16 I_{XX}} \tilde{p} \rho C_{RD} \quad (10)$$

$$\begin{aligned} \tilde{q}' = & 2 K_2 C_{NA} (\tilde{w} - \tilde{w}_w) L_{CGCP} + D \frac{K_2}{V} C_{MaM} \tilde{p} (\tilde{v} - \tilde{v}_w) L_{CGCM} + \\ & + D^2 K_2 C_{PD} \tilde{q} + D^2 K_2 C_{OM} - \frac{D}{V} \tilde{r} \frac{I_{XX}}{I_{YY}} \tilde{p} - \frac{D}{V} \tilde{r}^2 \tan \theta \end{aligned} \quad (11)$$

$$\begin{aligned} \tilde{r}' = & -2 K_2 C_{NA} (\tilde{v} - \tilde{v}_w) L_{CGCP} + D \frac{K_2}{V} \tilde{p} C_{MaM} (\tilde{w} - \tilde{w}_w) L_{CGCM} + \\ & + D^2 K_2 C_{PD} \tilde{r} - 2 D K_2 C_{OM} + \frac{D}{V} \tilde{p} \tilde{q} \frac{I_{XX}}{I_{YY}} + \frac{D}{V} \tilde{q} \tilde{r} \tan \theta \end{aligned} \quad (12)$$

III. MODIFIED PROJECTILE LINEAR THEORY

The projectile dynamics trajectory model consists of twelve highly first order ordinary differential equations, which are solved simultaneously by resorting to numerical integration using a 4th order Runge-Kutta method. In these equations to develop the modified projectile linear theory equations, the following sets of simplifications are employed: velocity \tilde{u} replaced by the total velocity V because the side velocities \tilde{v} and \tilde{w} are small. The aerodynamic angles of attack α and sideslip β are small for the main part of the atmospheric trajectory $\alpha \approx \tilde{w}/V$, $\beta \approx \tilde{v}/V$, also the yaw angle ψ is small so $\sin(\psi) \approx \psi$, $\cos(\psi) \approx 1$, and the projectile is geometrically symmetrical $I_{XY} = I_{YZ} = I_{XZ} = 0$, $I_{YX} = I_{ZZ}$ and aerodynamically symmetric. The wind velocity component \tilde{u}_w parallel to the projectile station line is negligible in comparison to the total velocity. The Magnus force components are small in comparison with the weight and aerodynamic force components and so they are treated as negligible. With the afore-mentioned assumptions, the expressions of the distance from the center of mass to the standard aerodynamic and Magnus centers of pressure are simplified. With the aforementioned assumptions, the above expressions results in:

$$x' = D \cos \theta \tag{13}$$

$$y' = D \cos \theta \psi \tag{14}$$

$$z' = -D \sin \theta \tag{15}$$

$$\tilde{u}' = -\frac{D}{V} g \sin \theta - K_1 V C_D \tag{16}$$

$$\tilde{v}' = -K_1 (C_D + C_{La}) (\tilde{v} - \tilde{v}_w) - D \tilde{r} \tag{17}$$

$$\tilde{w}' = \frac{D}{V} g \cos \theta - K_1 (C_D + C_{La}) (\tilde{w} - \tilde{w}_w) + D \tilde{q} \tag{18}$$

$$\tilde{p}' = D^5 \frac{\pi}{16 I_{XX}} \tilde{p} \rho C_{RD} \tag{19}$$

$$\begin{aligned} \tilde{q}' = & 2 K_2 (C_D + C_{La}) (\tilde{w} - \tilde{w}_w) L_{CGCP} + \\ & + D \frac{K_2}{V} C_{MaM} \tilde{p} (\tilde{v} - \tilde{v}_w) L_{CGCM} + \\ & + D^2 K_2 C_{PD} \tilde{q} + D 2 K_2 C_{OM} \end{aligned} \tag{20}$$

$$\begin{aligned} \tilde{r}' = & -2 K_2 (C_D + C_{La}) (\tilde{v} - \tilde{v}_w) L_{CGCP} + \\ & + D \frac{K_2}{V} \tilde{p} C_{MaM} (\tilde{w} - \tilde{w}_w) L_{CGCM} + \\ & + D^2 K_2 C_{PD} \tilde{r} - 2 D K_2 C_{OM} \end{aligned} \tag{21}$$

The equations 4, 5, 6 and 10 remain invariable. Modified linear trajectory model runs at faster time with variable aerodynamic coefficients than the corresponding full 6-DOF analysis. On the other hand 6-DOF gives results of high accuracy trajectory prediction.

IV. ATMOSPHERIC MODEL

Atmospheric properties of air, like density ρ , are being calculated based on a standard atmosphere from the International Civil Aviation Organization (ICAO).

V. INITIAL SPIN RATE ESTIMATION

In order to have a statically stable flight for spin-stabilized projectile trajectory motion, the initial spin rate \tilde{p}_o prediction at the gun muzzle in the firing site is important. According to McCoy definitions, the following form is used:

$$\tilde{p}_o = 2 \pi V_o / \eta D \text{ (rad / s)} \tag{22}$$

where V_o is the initial firing velocity (m/s), η the rifling twist rate at the gun muzzle (calibers per turn), and D the reference diameter of the projectile type (m). Typical values of rifling twist η are 1/18 calibers per turn for 105mm projectile. The 120 mm mortar projectile has uncanted fins, and do not roll or spin at any point along the trajectory.

VI. STATIC OR GYROSCOPIC STABILITY

Any spinning object will have gyroscopic properties. In spin-stabilized projectile, the center of pressure, the point at which the resultant air force is applied, is located in front of the center of gravity. Hence, as the projectile leaves the muzzle it experiences an overturning movement caused by air force acting about the center of mass. It must be kept in mind that the forces are attempting to raise the projectile's axis of rotation.

In Fig. 2, two cases of static stability are demonstrated: in the top figure, CP lies behind the CG so that a clockwise (restoring) moment is produced. This case tends to reduce the yaw angle and return the body to its trajectory, therefore statically stable. Conversely, the lower figure, with CP ahead of CG, produces an anti-clockwise (overturning) moment, which increases a further and is therefore statically unstable. It also possible to have a neutral case in which CP and CG are coincident whereby no moment is produced.

There is clearly an important correspondence in the distance between the center of pressure and the center of gravity and the center of the round. This distance is called the static margin. By definition, it is positive for positive static stability, zero for neutral stability and negative for negative stability.

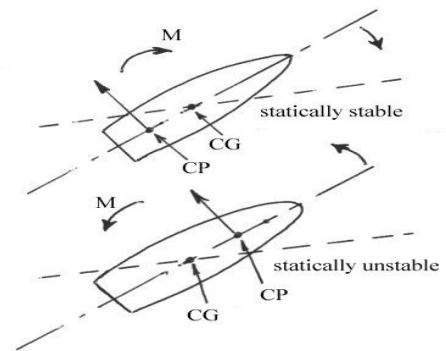


Figure 2. Static stability/instability conditions.

Firstly, we shall consider the case of a shell-like projectile in flight. This is initially flying at zero yaw incidence along its flight trajectory and is then struck by the gust of wind (figure 3) so that the nose is deflected upwards, producing a yaw angle (α). The response of the projectile to this disturbed yaw angle determines its stability characteristics. In particular, the initial response, determines whether it is statically stable or unstable.

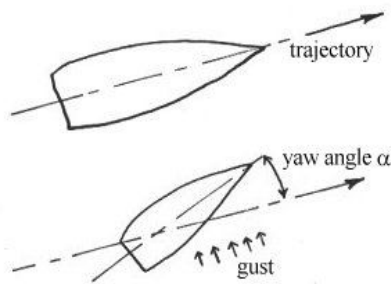


Figure 3. Gust Producing Yaw Angle on Projectile in Flight.

If the initial response is to move the nose back towards zero yaw (i.e. reducing the yaw angle) then it is statically stable. If the yaw angle initially increases as a response then it is statically unstable while if the disturbed yaw angle is retained the shell is neutral. It is therefore clear that it is the direction or sign of the resulting yawing moment generated that defines the static stability. This depends upon the aerodynamic force produced on the body due to the yaw angle and, in particular, upon the normal force (i.e. the aerodynamic force component perpendicular to the body axis) and the position at which it acts along the body's axis.

Classical exterior ballistics [1] defines the gyroscopic stability factor S_g in the following generalized form:

$$S_g = \frac{I_{XX}^2 \tilde{p}^2}{2 \rho I_{YY} S_{ref} DV^2 C_{OM}} \quad (23)$$

VII. COMPUTATIONAL SIMULATION

The flight dynamic models of 105 mm HE M1 and 120 mm HE mortar projectile types involves the solution of the set of the twelve first order ordinary differentials for two trajectories with variable aerodynamic coefficients, first the full 6DOF and second with simplifications for the modified trajectory, Eqs (4-6, 10, 13-20), which are solved simultaneously by resorting to numerical integration using a 4th order Runge-Kutta method.

Initial flight data	105 mm HE M1 projectile	120 mm HE Mortar projectile
x, m	0.0	0.0
y, m	0.0	0.0
z, m	0.0	0.0
φ, deg	0.0	0.0
θ, deg	15°, 30° and 45°	15°, 45° and 65°
ψ, deg	0.0	3.0
u, m/s	494.0	318.0
v, m/s	0.0	0.0
w, m/s	0.0	0.0
p, rad/s	0.0	0.0
q, rad/s	0.0	0.0
r, rad/s	0.0	0.0

The six-degree-o-freedom and the Modified linear model numerical trajectories were computed by using a time step size of $1.0 \times 10^{-3} s$, corresponding to dimensionless arc length $10D$, measured in calibers of travel. Initial flight conditions for both dynamic flight simulation models are illustrated in Table 2 for the examined test cases.

VIII. RESULTS AND DISCUSSION

The flight path of 6DOF trajectory motion [1] with variable aerodynamic coefficients of the 105 mm projectile with initial firing velocity of 494 m/sec, rifling twist rate 1 turn in 18 calibers (1/18), at 15°, 30° and 45°, are indicated in Fig. 2. The calculated impact points of the above no-wind trajectories with the proposed variable aerodynamic coefficients are compared with accurate estimations of modified linear trajectory analysis and provide quite good prediction of the entirety of the atmospheric flight motion for the same initial flight conditions.

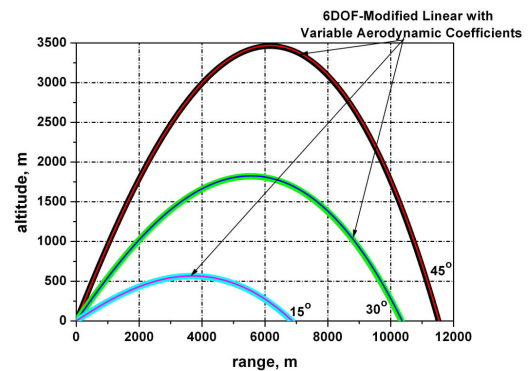


Figure 2. Trajectories of 105 mm projectile at pitch angles of 15, 30 and 45 degrees for 6DOF and Modified linear models.

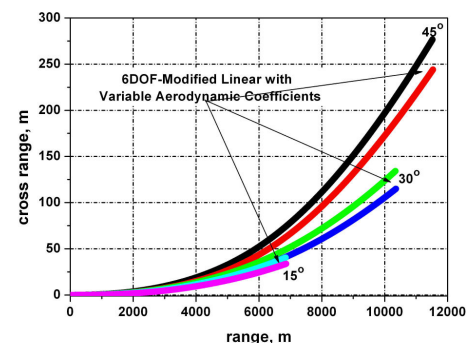


Figure 3. Cross range versus downrange distance of 105 mm projectile for Modified linear and 6DOF models.

Figure 3 shows cross range versus downrange distance for

both methods with no big differences in low launch angle but in high pitch angles. At 15, 30 and 45 degrees pitch angle we calculate cross ranges of 40 m, 134 m and 276 m, respectively, using the 6-DOF theory. For the same initial conditions the modified theory provides values 38 m, 120 m, and 250 m, respectively. Figure 4 shows that the two methods diagrams in velocity to range, at the 15, 30 and 45 degrees initial pitch angles has no differences. Also the figure 5 shows that the trajectories analysis for the three pitch angles are the same for the 105 mm spin stabilized projectile with variable aerodynamic coefficients.

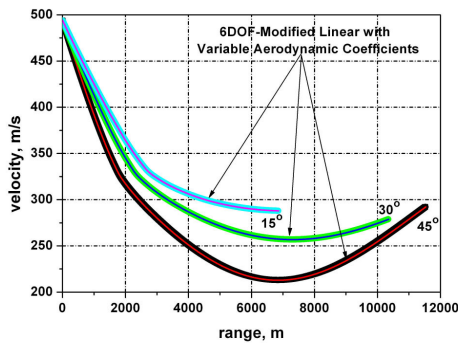


Figure 4. Velocity versus range of 105 mm projectile for low and high pitch angles in two trajectories models.

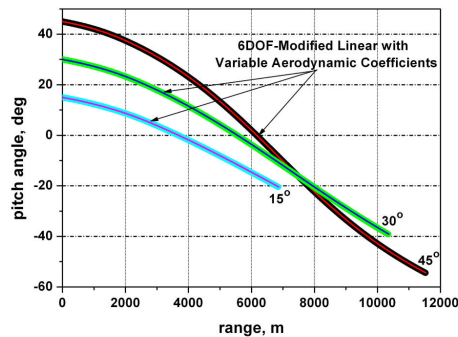


Figure 5. Pitch angles versus range of 105 mm projectile for Modified Linear and 6DOF models

The strong characteristics alterations of the total angle of attack influence the distributions of the most basic projectile trajectory phenomena taken into account constant aerodynamic coefficients during the completely atmospheric flight motion. Its effects are indicated in Fig. 6 for the 105 mm M1 projectile type fired from a 1/18 twist cannon with a muzzle velocity of 494 m/s at quadrant elevation angles of 45 and 70 degrees, respectively.

After the damping of the initial transient motion, at apogee, the stability factor for 45 degrees has increased from 3.1 at muzzle to 23 and then decreased to value of 8 at final impact point, as presented in Fig. 7. The corresponding flight behavior at 70 degrees initial pitch angle shows that the transient motion damps out quickly and the yaw of repose grows nearly 14

degrees at apogee, where the gyroscopic static stability factor has increased from 3.1 to 121 and then decreased to value of almost 6.6 at the impact area. Also in the circles Z_1 and Z_2 , there are two small angles, which interrupt the straight lines (crooked lines), because of the aerodynamic Magnus effect coefficient, and clearly varies with anything, which affects static margin. Therefore, any variations in the positions of either CP or CG will directly affect the value of C_{OM} . The position of CP will certainly vary during flight if the projectile passes through the transonic flow regime, due to complicated shock and expansion fan movements. In particular, it rises abruptly as the inverse C_{OM} term is highly reduced. This therefore means that S_g reduces under transonic conditions.

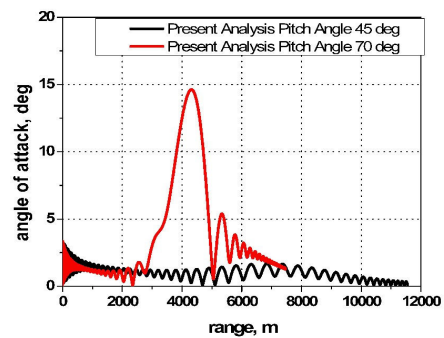


Figure 6. Comparative total angle of attack on the range of 105 mm projectile at 45 and 70 degrees.

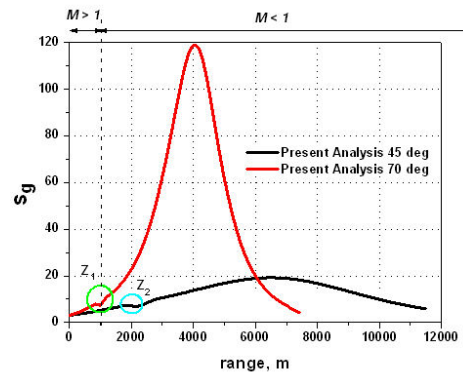


Figure 7. Comparative static stability variation at high and low quadrant angles for 105 mm projectile

The mortar projectile of 120 mm diameter is also examined for its atmospheric variable flight trajectories predictions in at pitch angles of 15°, 45°, and 65° with initial firing velocity of 318 m/s, and initial yaw angle 3°. The impact points of the 6DOF trajectories are compared with an accurately flight path prediction with the modified trajectory as presented in Fig. 8.

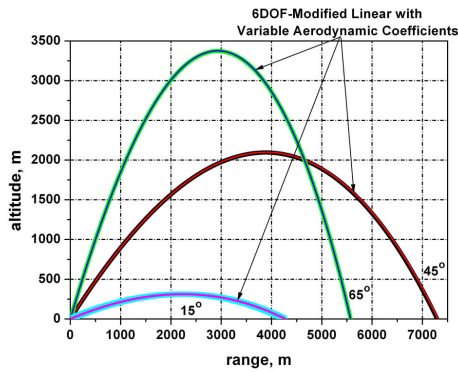


Figure 8. Flight paths of 120 mm projectile at pitch angles of 15, 45 and 65 degrees for 6DOF and Modified linear models.

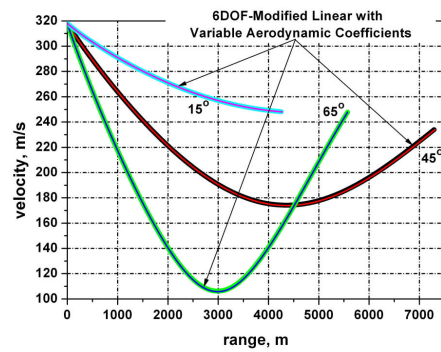


Figure 10. Velocity versus range of 120 mm projectile for low and high pitch angles in two trajectories models.

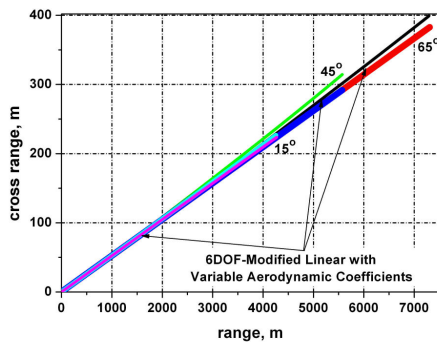


Figure 9. Cross range versus downrange distance of 120 mm projectile for Modified linear and 6DOF models

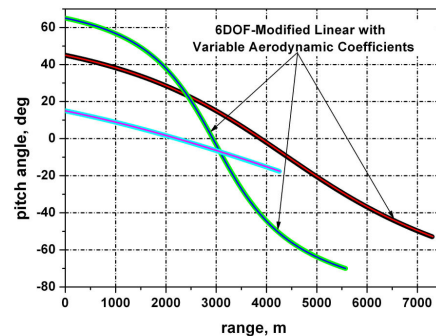


Figure 11. Pitch angles versus range of 120 mm projectile for Modified Linear and 6DOF models.

Figure 9 shows the cross range flight path of 120 mm projectile downrange distance for both methods with no big differences in low launch angle but in high angles. At 15, 45 and 65 degrees pitch angle for 6DOF with have the values of the cross range, 226 m, 400 m and 315 m, respectively. For the same initial conditions the modified theory has the values 226 m, 385 m, and 295 m, respectively.

Figure 10 shows that the two methods diagrams in velocity to range, at the 15, 45 and 65 degrees initial pitch angles has no differences. Also the figure 11 shows that the trajectories analysis for the three pitch angles is the same for the 120 mm mortar projectile with variable aerodynamic coefficients. The gyroscopic stability factor for the 120 mm projectile is zero because it is not spin in downrange distance.

A comparison of the times for the spin and fin stabilized projectiles showed the modified linear theory model computed the trajectory nearly twice as fast as the 6-DOF.

IX. CONCLUSION

Modified linear trajectory model was shown to provide reasonable impact predictions at short and long-range trajectories of high and low spin and fin-stabilized projectiles. Moreover, the Modified model showed some differences at cross range deflections, especially at high pitch angles. However, the comparison between 6-DOF and Modified trajectory model provided quite good results with the variable aerodynamic coefficients in whole flight path leading to low computation time suitable for rapid trajectory prediction. Criteria and analysis of gyroscopic stability are also examined.

This technique can be further coupled to a tracking control system for current and future control actions applied to fin and spin-stabilized projectiles for minimizing the estimated error to target impact area. The computational results of the proposed synthesized analysis are in good agreement compared with other technical data and recognized exterior atmospheric projectile flight computational models.

REFERENCES:

[1] McCoy, R., *Modern Exterior Ballistics*, Schiffer, Atten, PA, 1999.

[2] Fowler, R., Gallop, E., Lock, C., and Richmond H., "The Aerodynamics of Spinning Shell," *Philosophical Transactions of the Royal Society of London, Series A: Mathematical and Physical Sciences*, Vol. 221, 1920.

[3] Cooper, G., "Influence of Yaw Cards on the Yaw Growth of Spin Stabilized Projectiles," *Journal of Aircraft*, Vol.38, No. 2, 2001.

[4] Guidos, B., and Cooper, G., "Closed Form Solution of Finned Projectile Motion Subjected to a Simple In-Flight Lateral Impulse," AIAA Paper, 2000.

[5] Costello, M., and Peterson, A., "Linear Theory of a Dual-Spin Projectile in Atmospheric Flight," *Journal of Guidance, Control, and Dynamics*, Vol.23, No. 5, 2000.

[6] Burchett, B., Peterson, A., and Costello, M., "Prediction of Swerving Motion of a Dual-Spin Projectile with Lateral Pulse Jets in Atmospheric Flight," *Mathematical and Computer Modeling*, Vol. 35, No. 1-2, 2002.

[7] Cooper, G., "Extending the Jump Analysis for Aerodynamic Asymmetry," *Army Research Laboratory*, ARL-TR-3265, 2004.

[8] Cooper, G., "Projectile Aerodynamic Jump Due to Lateral Impulsives," *Army Research Laboratory*, ARL-TR-3087, 2003.

[9] Murphy, C., "Instability of Controlled Projectiles in Ascending or Descending Flight," *Journal of Guidance, Control, and Dynamics*, Vol.4, No. 1, 1981.

[10] Hainz, L., and Costello, M., "Modified Projectile Linear Theory for Rapid Trajectory Prediction," *Journal of Guidance, Control, and Dynamics*, Vol.28, No. 5, 2005.

[11] Etkin, B., *Dynamics of Atmospheric Flight*, John Wiley and Sons, New York, 1972.

[12] Joseph K., Costello, M., and Jubaraj S., "Generating an Aerodynamic Model for Projectile Flight Simulation Using Unsteady Time Accurate Computational Fluid Dynamic Results," *Army Research Laboratory*, ARL-CR-577, 2006.

[13] Amoruso, M. J., "Euler Angles and Quaternions in Six Degree of Freedom Simulations of Projectiles," Technical Note, 1996.

[14] Costello, M., and Anderson, D., "Effect of Internal Mass Unbalance on the Terminal Accuracy and Stability of a projectile," AIAA Paper, 1996.

A LIST OF SYMBOLS

C_X	= axial force aerodynamic coefficient
C_{NA}	= normal force aerodynamic coefficient
C_{MaF}	= magnus force aerodynamic coefficient
C_{RD}	= roll damping moment aerodynamic coefficient
C_{PD}	= pitch damping moment aerodynamic coefficient
C_{OM}	= overturning moment aerodynamic coefficient
C_{MaM}	= magnus moment aerodynamic coefficient
C_{MaF}	= magnus force aerodynamic coefficient
m	= projectile mass, kg

D	= projectile reference diameter, m
S	= dimensionless arc length
S_{ref}	= $\frac{\pi D^2}{4}$
V	= total aerodynamic velocity, m/s
$\tilde{u}, \tilde{v}, \tilde{w}$	= projectile velocity components expressed in the no-roll-frame, m/s
$\tilde{u}_w, \tilde{v}_w, \tilde{w}_w$	= wind velocity components in no-roll-body-frame, m/s
$\tilde{p}, \tilde{q}, \tilde{r}$	= projectile roll, pitch and yaw rates in the moving frame, respectively, rad/s
g	= gravity acceleration, m/s ²
I	= projectile inertia matrix
I_{XX}	= projectile axial moment of inertia, kg·m ²
I_{YY}	= projectile transverse moment of inertia about y-axis through the center of mass, kg·m ²
I_{XX}, I_{YY}, I_{ZZ}	= diagonal components of the inertia matrix
I_{XY}, I_{YZ}, I_{XZ}	= off-diagonal components of the inertia matrix
L_{CGCM}	= distance from the center of mass (CG) to the Magnus center of pressure (CM) along the station line, m
L_{CGCP}	= distance from the center of mass (CG) to the aerodynamic center of pressure (CP) along the station line, m
K_y^2	= non-dimensional transverse moment of inertia

GREEK SYMBOLS

α, β	= aerodynamic angles of attack and sideslip, deg
η	= rifling twist rate of the machine gun, calibers/turn
ρ	= density of air, kg/m ³
x, y, z	= projectile position coordinates in the inertial frame, m
φ, θ, ψ	= projectile roll, pitch and yaw angles, respectively, deg
K_1, K_2	= dimensional coefficients, $\pi \rho D^3 / 8m$ and $\pi \rho D^3 / 16I_{YY}$, respectively

SUBSCRIPTS

o	= initial values at the firing site
---	-------------------------------------

Dr Gkritzapis D.N. (1973) is Captain of Hellenic Police in Laboratory of Firearms and Tool Marks Section in Criminal Investigation Division, Athens, Greece, and graduated from the Department of Physics, School of Applied Sciences at the University of Patras, Greece.

He is a PhD holder in Mechanical Engineering and Aeronautics Department, at University of Patras, for thesis of 'Exterior Ballistics'. He took part in Atmospheric Flight Mechanics Conference and Exhibit, AIAA, on Hilton-Head, South Carolina on August 2007. And also he was at the conferences of World Scientific and Engineering Academy and Society and at World Academy of Sciences, Engineering and Technology, in the International Conference of Numerical analysis and Applied Mathematics, in the International Conference on Avionics Systems / Guidance and Control Systems Design and Simulation (Uav & Civil Aircraft), and at the end, he took part in other three International conferences in Greece. His papers were acceptance of the Open Mechanics Journal, Journal of Pyrotechnics, Journal of Battlefield Technology, International Journal of Mathematical, Physical and Engineering Sciences, Journal of Wseas Transactions on Information Science and Applications, Journal of Engineering Science and Technology Review and in International Review of Aerospace Engineering.

Dr Gkritzapis D. is member of AIAA, and the Society of Hellenic Physicists.

Dr. Panagiotopoulos E.E. (1980) is a Ph.D holder in Mechanical Engineering and Aeronautics Department at University of Patras. His postgraduate studies were started during the period 2002-2003 in the aerospace technology field. In his PhD thesis is dealing with the prediction of nominal entry descent flight path trajectories including real gas flow phenomena and modelling the particular conditions of the most basic planetary atmospheres. The last fatal flight of Columbia Space Shuttle in 1st February 2003 shows the great importance of a refined aerothermodynamic analysis of entry trajectories in Earth (or other basic planetary) atmospheres.

Furthermore, is interested in the scientific field of exterior ballistics atmospheric motions in addition to the complicated nonlinear aerodynamic phenomena for big and small projectile types. He is participating in over 15 international conferences on the above scientific areas and his papers were acceptance of the Open Mechanics Journal, Journal of Pyrotechnics, Journal of Battlefield Technology, International Journal of Mathematical, Physical and Engineering Sciences, Journal of Wseas Transactions on Information Science and Applications, Journal of Engineering Science and Technology Review and in International Review of Aerospace Engineering.

He is member of EUROAVIA and TCG (Technical Chamber of Greece).